Vacuum Packaging Sensor Based on Time-Resolved Phosphorescence Spectroscopy

Esmaeil HEYDARI*, Fatemeh YARI, and Hossein ZARE-BEHTASH

Nanophotonic Sensors & Optofluidics Lab, Faculty of Physics, Kharazmi University, Tehran 15719-14911, Iran

*Corresponding author: Esmaeil HEYDARI E-mail: e.heydari@khu.ac.ir

Abstract: Intelligent food packaging with the multisensory analysis is promising as the next generation technology of food packaging. The oxygen content in food packaging is one of the crucial parameters affecting the food quality and shelf life. Caviar is among the most nutritious and costly food sources. Here, a photonic oxygen-sensing system, based on the time-resolved phosphorescence spectroscopy of a platinum complex, is developed for non-contact, non-intrusive, and real-time vacuum packaging quality control, and implemented for caviar packaging. The sensor is embedded in protective polyethylene layers and excited with a short-pulsed light emitting diode (LED) source. Integration of a blue pulsed light source, a fast and amplified silicon photodiode controlled by the Spartan-6 field programmable gate array (FPGA), and a long lifetime platinum complex results in a photonics-based oxygen sensor with a fast response and high sensitivity to the vacuum packaging damage, which is suitable for caviar. It is revealed that applying the polyethylene layers protects the caviar from the platinum complex, leaching while not interfering with the sensor functionality. Characterizing the photonic system based on its sensitivity, repeatability, stability, and long-term operation demonstrates its capability for this application.

Keywords: Caviar; photoluminescence lifetime; oxygen sensor; platinum porphyrin complex; vacuum packaging

Citation: Esmaeil HEYDARI, Fatemeh YARI, and Hossein ZARE-BEHTASH, "Vacuum Packaging Sensor Based on Time-Resolved Phosphorescence Spectroscopy," *Photonic Sensors*, 2024, 14(1): 240120.

1. Introduction

Nowadays, there is tremendous interest in technologies that make food packaging smart, because the expiration date on the package does not guarantee or provide information on the quality of packaging, transport, and storage of the product [1]. Moreover, even if all the standard regulations are followed, the lack of real-time information on the food status may leave consumers at risk due to foodborne illnesses [2]. Traditionally, a food package, as a passive barrier, primarily helps to protect food from environmental parameters, such as moisture, light, oxygen (O_2), microbes, chemical and mechanical stresses, and dust [3].

In recent decades, due to the growing interest of the final consumers in the freshness, quality, and safety assurance, two main strategies have been pursued to enhance the current packaging systems, namely, active and intelligent packaging [4]. Active packaging is realized by applying additives, such as gas scavengers, temperature controllers, moisture controllers, and antimicrobial and antioxidant-releasing components to increase the food quality and prolong its shelf-life. Vacuum and modified atmosphere packaging (MAP) technologies are the

Received: 5 January 2023 / Revised: 6 June 2023

DOI: 10.1007/s13320-023-0692-y
Article type: Regular

most commonly used concepts in active packaging [5]. Intelligent packaging is a packaging system that continuously reports the parameters of a product to the customer throughout the supply chain based on the ability of sensing, detecting or recording the external/internal changes in the product [6]. The main concepts in intelligent packaging are indicators or sensors. Indicators often exhibit qualitative information about packaged food based on a visible color change [7]. For instance, the UV-activated O_2 indicator inks usually contain redox dyes, electron donors, UV-absorbing photocatalysts, and polymers [8], which in the absence of O_2 lose their color, and in the presence of O_2 gain color [9]. Unlike the indicator systems, photonics-based O_2 sensors provide a prompt, reversible, and quantitative response to the non-destructive headspace analysis of the packaged food. Among them, photoluminescence (PL)-based O_2 sensors are the most advanced [10, 11]. The easy access of the photonic sensors to the packaging atmosphere, availability of the measurement tools, and protection of the sensor from the atmosphere outside the package are important requirements for integrating the sensors [12]. The membrane of these sensors consists of a phosphorescent oxygen-sensitive probe (POSP) embedded in a polymeric or sol-gel matrix [13, 14]. Commonly used the POSP includes a metal-organic complex of platinum (II), palladium (II) porphyrins, and ruthenium (II) since they exhibit a long lifetime, high O_2 sensitivity, a high molar extinction coefficient, excellent quantum yields, and long photostability [15, 16]. They have several significant advantages over other systems [17, 18], such as no O_2 consumption during measurement and non-invasive and contactless measurement in a sealed container. In addition, these sensors are affordable, disposable, easily miniaturized, and calibration-free. As a result, they can be used on a large scale. These sensors provide accurate and fast responses in real time [19, 20].

The most important criteria for selecting O_2 sensors used for packaging applications are the planar shape of the sensing platform for the ease of integration, suitable solvent for low toxicity and fast evaporation, preventing leaching of the complex, insensitivity to the moisture, photostability, and long shelf-life stability. The application of an O_2-permeable film laminated on top of the sensor, between the sensor and the food product, prevents the migration of the sensor's components into the food, which is vital from the food safety perspective. The POSP usually relies on the collisional quenching of the excited metal-organic complex by O_2 molecules, which decreases the emission intensity and corresponding lifetime depending on the O_2 concentration. The POSP molecules have a long emission lifetime than fluorescent dye molecules. As a result, they are more likely to interact with the O_2 molecules, thus reducing their emission intensity and lifetime accordingly [21]. In a homogeneous microenvironment, the O_2 quenching process usually follows the Stern-Volmer equation:

$$I_0/I = \tau_0/\tau = 1 + K_{SV}[O_2] \quad (1)$$

where I_0 and τ_0 are the unquenched luminescence intensity and lifetime at the O_2 concentration of zero, I and τ are the intensity and lifetime at the measured state, K_{sv} is the Stern-Volmer quenching constant, and $[O_2]$ is the O_2 partial pressure [22]. The initial characterization for food packaging applications involves plotting the sensors' lifetime or intensity ratio based on the O_2 concentration to obtain a reproducible calibration function. Also, the sensitivity of these sensors varies based on the environmental temperature; therefore, calibration functions must be corrected based on the food packaging's temperature. Also, the sensor performance must be investigated through a comprehensive evaluation of the stability, reversibility, and repeatability to determine the POSP characteristics [23, 24]. The PL intensity is influenced by the factors, such as the fluctuation in the excitation light source, detector drift, optical

path, degradation or leaching of the metal-organic complex, thickness of the POSP, and concentration of the dye in the POSP. Instead, the PL lifetime is immune to the mentioned factors because it is an intrinsic property of the POSP. The time-domain and frequency-domain modes are commonly used to measure the PL lifetime. In the frequency-domain mode, the optical source is a sinusoidally modulated light at a fixed frequency, producing a modulated PL emission signal. The PL signal exhibits a phase shift corresponding to the PL lifetime that can be measured. In the time-domain mode, the POSP is excited by short light pulses. Then, the PL intensity decays exponentially, and the decay curve is fitted with an exponential function to calculate the PL lifetime, which exhibits better performance than frequency-domain sensors [25–27]. In recent years, O_2 sensors using the platinum octaethyl porphyrin ketone (PtOEPK) complex have been adopted to track O_2 levels in the cheddar cheese [28], bread [29], and chicken [30] packages utilizing the frequency-domain technology and in salad packages using the time-domain technology [31]. In another study, using the time-domain technology, an O_2 sensor comprising of the platinum benzoporphyrin (PtBP) complex, was used to track O_2 levels in meat packages [32].

Eggs separated from the ovaries of various sturgeons are commonly called caviar. They are used as energetic and nutritious food in many parts of the world [33]. The most valuable type of caviar is obtained from wild sturgeons, which for instance, are found in the Caspian Sea region, including beluga (huso huso), asetra (acipenserpersicus), and sevruga (acipenserstellatus) caviars [34, 35]. The caviar contains high levels of lipids, phospholipids, long-chain polyunsaturated fatty acids (PUFA) [36], proteins [37], vitamin A, and B-complex vitamins [38]. Since the caviar contains a high percentage of proteins (22%–28%) and lipids (15%–78%), in addition, it does not go under pasteurization during processing, and the potential for microbial and chemical spoilage is high [39].

The caviar is packed under the vacuum condition, which effectively removes the possible biological and chemical contaminants from the surrounding environment [40]. However, factors, such as the poor air evacuation, poor sealing, exchange between O_2 trapped within the caviar eggs and the package headspace, and damage to the packaging during the vacuum packaging (VP) process or during transport and storage, can lead to O_2 leaking into the package [41] and cause the oxidation of lipids, and decomposition of proteins and discoloration. This in turn, creates an optimal condition for the growth and activity of all aerobic microorganisms that spoil the caviar [42]. Oxidation also reduces the caviar's nutritional value and changes the sensory properties such as the taste, texture, and aroma [43]. Thus, an accurate evaluation of the O_2 levels within the VP caviar packages makes it possible to identify the damaged packages and take the necessary steps [44].

In this paper, we develop a photonics-based O_2 sensor system for the caviar vacuum packaging quality control by integrating a composite of platinum meso-tetra (pentafluorophenyl) porphyrin (PtTFPP) in a polystyrene (PS) matrix embedded in two O_2-permeable polyethylene layers with the high- and low-density, and a nanosecond pulsed light emitting diode (LED) with an amplified photodiode controlled by a field programmable gate array (FPGA) microcontroller. This sensor is implemented for real-time, non-intrusive, and contactless O_2 detection in caviar packages based on the time-resolved phosphorescence spectroscopy. The probe functionally is investigated through a comprehensive evaluation of the sensitivity, stability, reversibility, and repeatability. Finally, by embedding this sensor in vacuumed caviar packages, we demonstrate that it is possible to distinguish the damaged packages precisely based on the O_2 concentration.

2. Materials and methods

Fabrication of the POSP film: the PtTFPP, polystyrene, toluene solvent (99.9%), and

polyethylenes were purchased from Frontier Scientific, Sigma-Aldrich, Merck, and A.K.P.C, respectively. A solution was prepared by dissolving 2 mg of platinum meso-tetra (pentafluorophenyl) porphyrin powder, as an oxygen-sensitive complex, in 500 μL of toluene as a solvent. Then, 0.2 g of polystyrene was dissolved, as the oxygen permeable matrix, in 1 mL of toluene. The solutions were thoroughly mixed using a magnetic stirrer at room temperature for 1 h to make a homogeneous solution. Subsequently, 50 μL of each solution was poured into a vial and placed on a magnetic stirrer for 30 min. Finally, to make a circular film with a diameter of 8 mm, the solution was poured onto a glass slide, annealed overnight in an oven at 75 ℃, and punched with a biopsy punch.

Instrumentation: the absorption spectrum was measured using Analytik Jena Specord 210 Plus. A Thorlabs CCS100 spectrometer was used for PL spectral analysis. A nanosecond pulsed LED with a wavelength of 450 nm was used as a source of excitation. The OSRAM SFH2704 silicon photodiode, with the dimensions of 1×1 mm^2, accompanied by OPA354 and AD8042 rail-to-rail amplifiers, were used to detect the PL lifetime. The Spartan-6 FPGA from XILINX controlled all the electronic components. The Lutron YK-22DOA O_2 meter was used to measure the O_2 concentration in the air. DHT11 temperature and humidity sensors in combination with Arduino Uno were used to measure the temperature and humidity. The Spectro ARCOS system and Varian ICP-OES 730-ES ICP-OES were used for analyzing the PtTFPP leaching.

Calibration setup: the POSP was placed inside a temperature and gas-controlled plexiglass chamber to investigate its work function. The chamber had an inlet to supply N_2 gas and a Lutron reference O_2 sensor to monitor the O_2 percentage. The N_2 gas was then injected into the measurement chamber until the O_2 concentration reached 0%, monitored by the reference oxygen meter. Then, the N_2 injection stopped, and the PL lifetime values were recorded for the oxygen concentration in a wide range from 0% to 20.9%.

3. Results and discussion

Figure 1 illustrates the schematic demonstrations of the photonics-based O_2 sensor developed for the caviar vacuum packaging quality control and the corresponding detection mechanism. The POSP is optically excited with a nanosecond pulsed LED light source. Subsequently, excited POSP molecules are transitioned from the singlet to triplet states via intersystem crossing (ISC). The collision of the triplet-state molecular O_2 with the excited POSP molecules results in non-radiative energy transferring to the O_2 molecules. Therefore, it leads to PL quenching of the excited POSP, which appears as a decrease in the PL lifetime. In addition, the higher the molecular O_2 concentration is, the greater the likelihood that the platinum complex film interacts with the O_2 is, resulting in a higher level of lifetime quenching. The absorption spectrum of the POSP film, comprising the PtTFPP complex doped in a PS matrix, was measured by a spectrometer to determine the excitation wavelength. This spectrum enables us to select a suitable LED light source to excite the POSP optically. The absorption spectrum of the POSP is presented in Fig. 2(a) with a blue-green color showing three peaks at 392 nm, 510 nm, and 540 nm. Therefore, a 450-nm blue LED light source with the power of 4 W was selected for the POSP excitation. The PL spectrum was measured using a CSS100 spectrometer, and the measurement time was set to 1 000 ms. The PL spectrum is illustrated in Fig. 2(a) in red, with a maximum at 652 nm. Figure 2(b) shows the time-resolved PL decay of the POSP when it was excited with the LED pulses for two different arbitrary O_2 concentrations at the temperature of (22.0 ± 0.1) ℃. According to the results, the PL intensity decays exponentially. The decay curve was fitted with a one-term exponential function using the Levenberg Marquardt algorithm to extract the lifetime of the POSP.

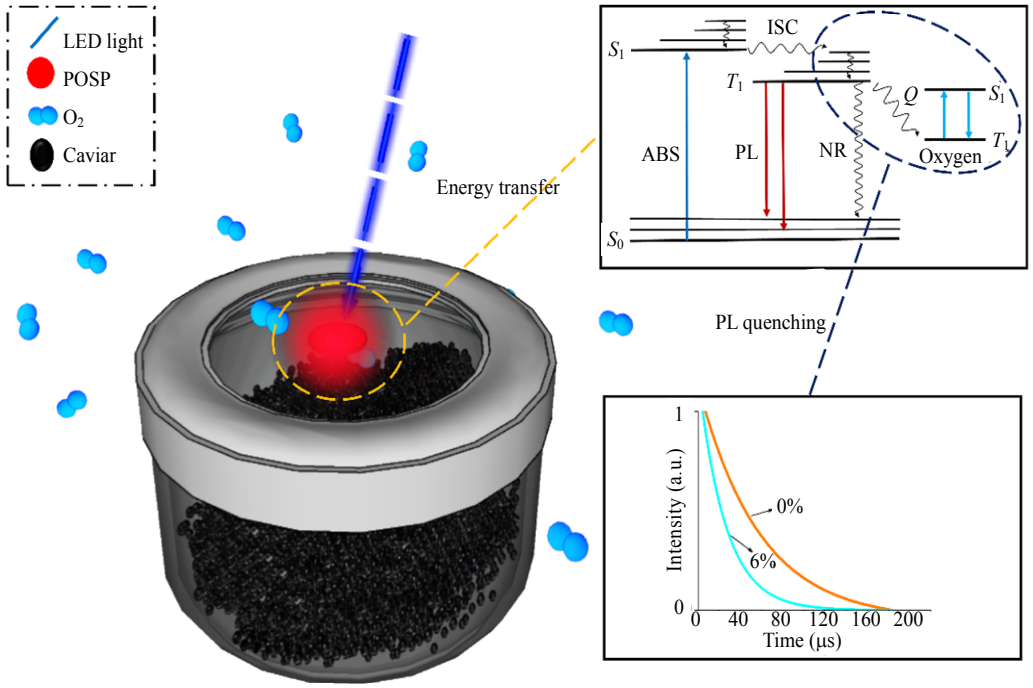

Fig. 1 Concept of the photonic sensor for caviar vacuum packaging quality control: energy diagram for energy transfer between the POSP and O_2 molecules and the corresponding changes in the photoluminescence lifetime.

For instance, in Fig. 2(b), the lifetime decreases from 53.5 μs to 35.8 μs as the O_2 concentration increases from 0% to 3.0% because as the O_2 concentration is increased, the likelihood that the excited POSP interacts with the O_2 molecules and non-radiative energy transferring to the O_2 takes place is higher, resulting in a higher level of lifetime quenching. The time-resolved PL spectroscopy setup for O_2 measurement is demonstrated in Fig. 2(c). The POSP was excited with multiple 50 ns pulses of the blue LED. The LED light was focused after passing a convex lens with the focal length of 1 cm to excite the POSP efficiently. The same lens collected the PL emission and guided it through a red filter to prevent the LED light from reaching the SFH2704 silicon photodetector (PD). Then, the PD signal was amplified by combining the OPA354 and AD8042 amplifiers. Afterward, the amplified analog signal was converted to digital data. Spartan-6 FPGA was employed to control all electronic components. All data were sent to a computer to be fitted with the one-tern exponential function in order to calculate the lifetime. A LabVIEW program was developed for the data acquisition and analysis. Figure 2(d) shows the concept that a multipulse LED source for the excitation of the POSP, with multiple 50-ns pulses and a total width of 45 μs, is adjusted for efficient excitation.

The critical parameter of the POSP in food packaging applications is the sensitivity diagram which involves plotting the sensor's Stern-Volmer lifetime ratio (τ_0/τ) based on the O_2 concentrations in the working range of 0.0% to 20.9%, resulting in a reproducible calibration function. Figure 3(a) shows the lifetime ratio based on the O_2 concentrations, where each point represents an average value of three times of consequent measurement, while the temperature was maintained at (24.0 ± 0.1) ℃. The results demonstrate that the observed behavior of the Stern-Volmer diagram is linear in the O_2 concentration range of 0.0% to 20.9%. Therefore, the acquired data were fitted with a linear function in which the slope value was the Stern-Volmer constant. The sensitivity slope was calculated as 0.15. The graph's linearity indicates that the

dispersion of the PtTFPP molecules inside the matrix is almost homogeneous. In addition, the higher the molecular O_2 concentration is, the lower the PL lifetime is. The stability evaluation of the PL lifetime was performed per every 1 min in a chamber at the O_2 concentration, temperature, and duration of 20.9%, 24.1 ℃–24.5 ℃, and 90 min, respectively.

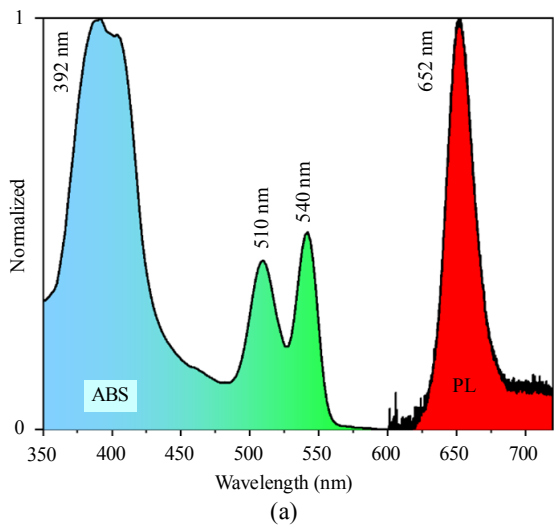

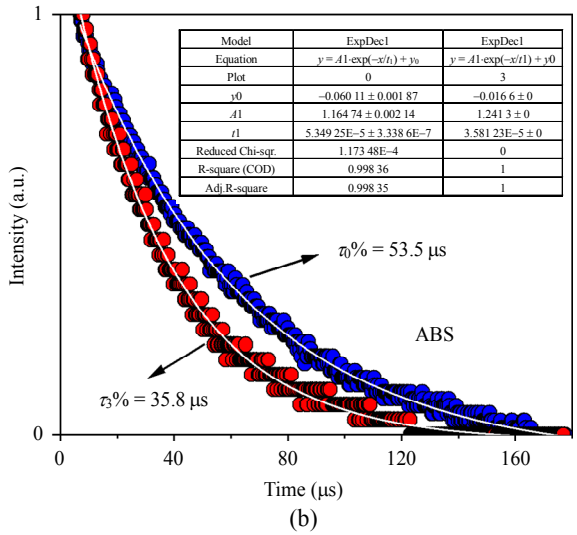

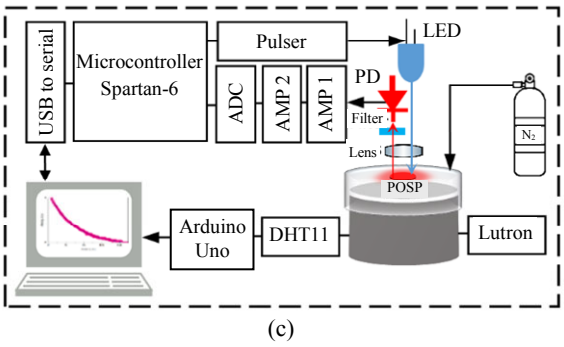

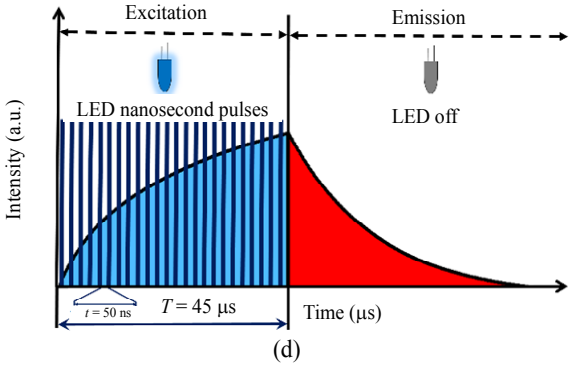

Fig. 2 Time-resolved phosphorescence spectroscopy for oxygen sensing: (a) absorption and PL spectra of the POSP, the absorption spectrum peaks are located at 392 nm, 510 nm, and 540 nm. The emission peak is at 652 nm, (b) time-resolved PL spectroscopy of the excited POSP at two different O_2 concentrations. Red represents the 3.0% and blue color the 0.0% O_2 concentration at (22.0 ± 0.1) ℃, (c) measurement setup of O_2 concentration using the time-resolved PL spectroscopy, and (d) concept of the multipulse LED source for excitation of the POSP (ADC: analog to digital converter and AMP: amplifier).

In Fig. 3(b), the PL lifetime is plotted against time to evaluate the stability of the POSP. A PL stability of 99% was obtained, which shows that the POSP exhibited excellent lifetime stability for the caviar vacuum packaging quality control. The POSP's limit of detection was 0.2%. Next, the sensor reversibility, which is the ability to perform measurement multiple times, was obtained by calculating the relative standard deviation (RSD). Figure 3(c) shows the result of the reversibility test where the O_2 concentration varies several times between 0.0% and 5.3%. Each point represents an average value of the three consequent measurement times, and the temperature was maintained between 24.3 ℃ and 24.5 ℃. The RSD values were 0.1% and 0.6% at the O_2 concentrations of 0% and 5.3%, respectively. The RSD value for 0% O_2 is lower than that for the 5.3% since at lower concentrations of O_2, the emission intensity is higher, and therefore, the signal-to-noise ratio is higher. Thus, POSP exhibits the excellent reversibility. The high level of the reversibility is indicative of the reliability of the measurement. In addition, the PL lifetime was

measured for the temperature range of 10.0 ℃ – 35.0 ℃ to obtain its effect on the sensor's work function. Figure 3(d) depicts the temperature-dependent lifetime variation, where each point represents an average value of three times of consequent measurement. According to the figure, the lifetime decreases by increasing the temperature due to a higher level of collisional relaxation at higher temperatures, and the POSP exhibits a linear response with the slope of 0.2.

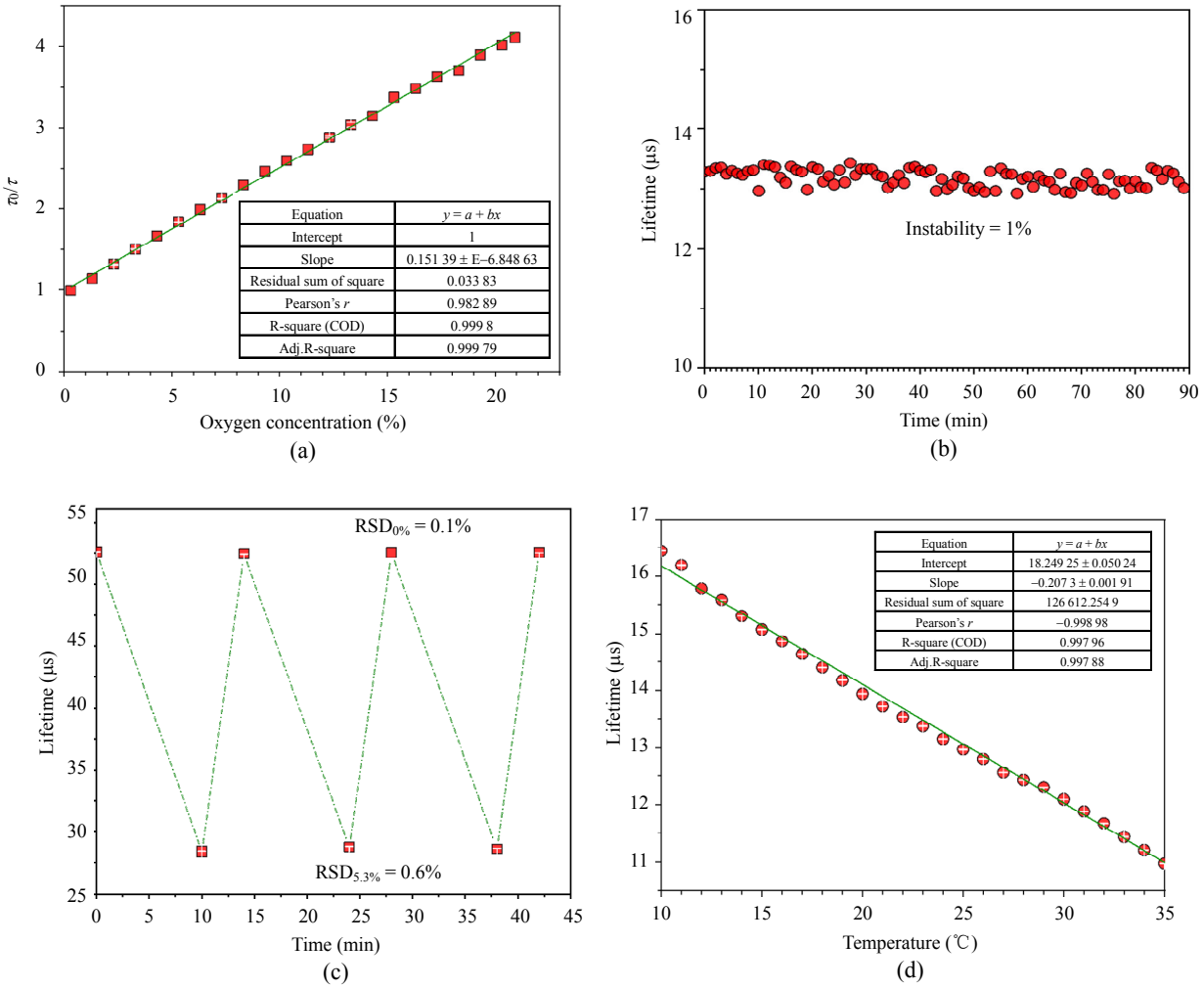

Fig. 3 Calibration and characterization of the POSP: (a) Stern-Volmer lifetime ratio versus O_2 concentration at (24.0 ± 0.1) ℃, (b) stability of the POSP at 20.9% O_2 concentration, (c) repeatability of the POSP for modulation between 0.0% and 5.3% O_2 concentration, and (d) temperature-dependent lifetime variation.

Three identical POSPs were prepared to test the sensor-to-sensor repeatability. The O_2 concentration was varied from 1.0% to 20.9% to compare their responses. Figure 4(a) shows their responses where the red circles, green triangles, and blue squares correspond to samples 1, 2, and 3, respectively. According to the results, the overlap of these three POSPs represents their excellent repeatability. Figure 4(a) inset presents the three samples.

After obtaining the optical characterization of the POSP, it was used for the quality control of caviar vacuum packaging. Thus, the POSP was laminated between a high-density polyethylene (HDPE) layer and a low-density polyethylene (LDPE) layer with a thickness of 100 μm to prevent PtTFPP from leaching into the caviar. The HDPE and LDPE were inside and outside layers correspondingly. LDPE is transparent, so it allows for the excitation of the POSP with an LED. HDPE exhibits humidity resistance, and hence, it was

placed with the direct contact with the caviar [45, 46]. Figure 4(b) depicts the setup drawn in Fig. 2(c) used for the Beluga caviar vacuum packaging control, the sandwiched POSP applied to the caviar packaging, and its corresponding structure.

Next, the effect of applying the polyethylene layers was investigated on the optical function of the POSP. First, the bare POSP was placed in direct contact with the caviar packaging atmosphere, and the O_2 level was modified from 20.9% to 0%. Next, the POSP layer was embedded between the two layers of HDPE and LDPE, and a similar experiment in the caviar packaging was repeated. Figure 4(c) shows that there is approximately a 215-s time delay between the sandwiched POSP and the bare POSP to reach from 20.9% to 0% O_2 concentrations in the same condition. This implies that the polyethylene layers introduce a negligible delay in reducing the penetration rate of the O_2 molecules while protecting the caviar and POSP itself.

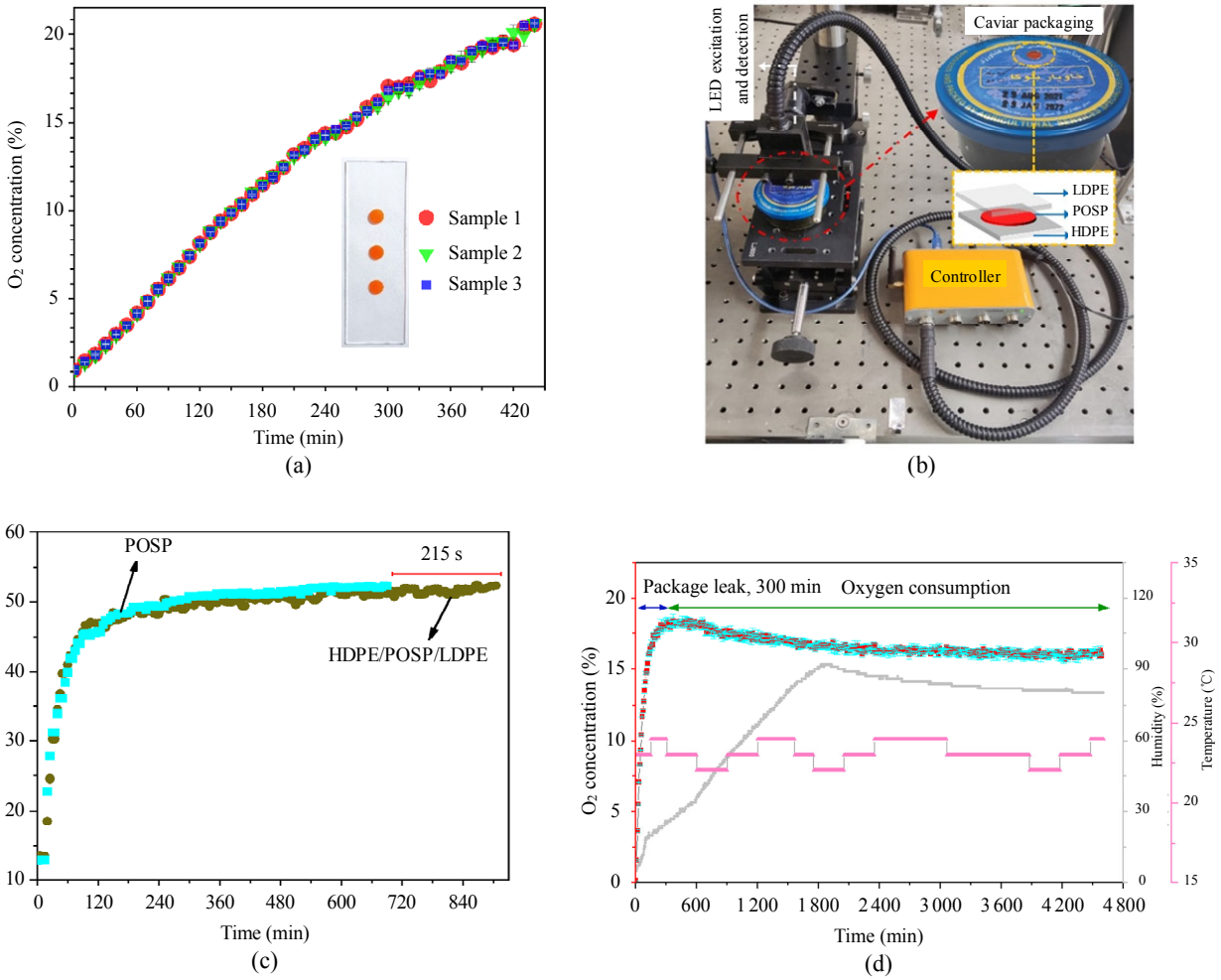

Fig. 4 Application of the POSP for contactless, non-intrusive, and real-time measuring the oxygen concentration in the caviar packaging: (a) sensor to sensor repeatability, (b) real measurement setup and the POSP structure includes LDPE, POSP, and HDPE layers, (c) effect of protective layers on the POSP in the caviar packaging: cyan squares correspond to the POSP alone, and the dark-green circles to HDPE/POSP/LDPE, and (d) real-time measurement of the oxygen concentration, humidity, and temperature in the caviar packaging: red squares correspond to the O_2 concentration, gray squares correspond to the humidity, the pink squares correspond to the temperature, and cyan lines correspond to error bars of measurement.

The long-term capability of the sensor was investigated by attaching the POSP into the gas- and temperature-controlled chamber containing 5 g of caviar and a DHT11 temperature and humidity sensor for long-term monitoring, when the packaging suffered from leakage. The temperature

varied between 22.0 ℃ and 24.0 ℃ during the test. Initially, the O_2 concentration of the chamber reached 0% by injecting N_2 gas. Afterwards, the O_2 level inside the chamber gradually increased from 0% to 18.5% within 512 min, according to Fig. 4(d). The chamber was then sealed at 18.5% to demonstrate the capability of the POSP to detect minor changes in the O_2 level. The O_2 level was measured for the next 68 h with an 8-min time interval. Figure 4(d) shows the O_2 levels start to decrease due to the adsorption of O_2 by the caviar until it reaches approximately 15.9%. The suitable temperature for keeping caviar is between –3 ℃ and 3 ℃, and heat accelerates the oxidation process of lipids and proteins [47]. Lopez *et al.* [48] reported that when the caviar was exposed to O_2, the PUFAs content oxidized, and this process led to a taste bitter. Molds, yeasts, and aerobic bacteria need O_2 and a temperature of 35 ℃, to survive, grow, and reproduce. The spoilage process begins at the top layer, which is most exposed to O_2. The molds and yeasts grow exponentially, increasing the O_2 uptake into the atmosphere over time. The amount of active water and moisture content in the caviar is high; therefore, the molds and yeasts absorb the oxygen-containing moisture of the caviar during the growth and reproduction process. At the end of the spoilage process, the caviar grains almost dry out, and its texture changes, and the humidity inside the chamber reaches approximately 80% ± 5%. Thus, the O_2 POSPs can be used to evaluate the efficiency of large-scale vacuum packaging and quantify the quality control parameters for the O_2 content in these packages. Due to the nature of this thin layer, it can be easily included in food packaging.

It is essential to be confident that there is no leaching from the POSP to the package content, and therefore, inductively coupled plasma optical emission spectroscopy (ICP-OES) was employed [49, 50]. Thus, three samples were prepared and kept in a 3 mL aqueous medium for 120 h. The first sample contained control water, the second sample contained sandwiched POSP soaked in water, and the third sample contained 2 mg PtTFPP powder mixed in water. The Spectro ARCOS system detected no trace of the PtTFPP in the first two samples with a limit of detection (LOD) of 0.02 ppm. A similar test was carried out after 24 h incubation of samples using Varian ICP-OES 730-ES with 0.01 ppm LOD, and again no trace of PtTFPP was detected for the first two samples. As a result, the polyethylene layers are reliable barriers in protecting the caviar from leaching the platinum complex.

4. Conclusions

In this paper, a photonics-based oxygen sensor was developed for caviar vacuum packaging quality control by integration of a nanosecond LED light source, fast and amplified photodetector, FPGA microcontroller, and PtTFPP-PS POSP embedded in the oxygen-permeable HDPE and LDPE layers for real-time, precise, and non-contact detection. The time-resolved phosphorescence spectroscopy was used for lifetime measurement, which is more accurate than the conventional phase-detection approach. The pulsed LED light sources are preferred over laser light sources due to their low cost, accessibility, small size, and durability. Two layers of HDPE and LDPE were employed to avoid possible leaching of the PtTFPP, and through a series of experiments, no trace of PtTFPP was found. It was shown that these layers had a negligible impact on the sensor's response time while protecting the caviar and the sensor itself. It was demonstrated that the sensor system exhibited excellent sensitivity, stability, reversibility, and repeatability through systematic tests.

Acknowledgment

The authors would like to thank Dr. Reza SHAHIFAR from Agriculture Services Specialized Holding Company, Iran for providing the caviar samples and Small Industries and Industrial Parks Organization, Iran for its support.

Declarations

Conflict of Interest The authors declare that they have no competing interests.

References

[1] O. Hrytsenko, V. Shvalagin, G. Grodziuk, and V. Granchak, "Influence of parameters of screen printing on photoluminescence properties of nanophotonic labels for smart packaging," *Journal of Nanotechnology*, 2017.

[2] H. Yousefi, H. M. Su, S. M. Imani, K. Alkhaldi, C. D. Filipe, and T. F. Didar, "Intelligent food packaging: A review of smart sensing technologies for monitoring food quality," *ACS Sensors*, 2019, 4(4): 808–821.

[3] P. Puligundla, J. Jung, and S. Ko, "Carbon dioxide sensors for intelligent food packaging applications," *Food Control*, 2012, 25(1): 328–333.

[4] P. E. Araque, I. M. Pérez de Vargas Sansalvador, N. L. Ruiz, M. M. Erenas, M. A. C. Rodríguez, and A. M. Olmos, "Non-invasive oxygen determination in intelligent packaging using a smartphone," *IEEE Sensors Journal*, 2018, 18(11): 4351–4357.

[5] C. A. Kelly, M. Cruz-Romero, J. P. Kerry, and D. B. Papkovsky, "Stability and safety assessment of phosphorescent oxygen sensors for use in food packaging applications," *Chemosensors*, 2018, 6(3): 38.

[6] S. Kalpana, S. R. Priyadarshini, M. Maria Leena, J. A. Moses, and C. Anandharamakrishnan, "Intelligent packaging: trends and applications in food systems," *Trends in Food Science and Technology*, 2019, 93: 145–157.

[7] K. Won, N. Y. Jang, and J. Jeon, "A natural component-based oxygen indicator with in-pack activation for intelligent food packaging," *Journal of Agricultural and Food Chemistry*, 2016, 64(51): 9675–9679.

[8] C. H. T. Vu and K. Won, "Novel water-resistant UV-activated oxygen indicator for intelligent food packaging," *Food Chemistry*, 2013, 140(1–2): 52–56.

[9] C. H. T. Vu and K. Won, "Leaching-resistant carrageenan-based colorimetric oxygen indicator films for intelligent food packaging," *Journal of Agricultural and Food Chemistry*, 2014, 62(29): 7263–7267.

[10] S. Banerjee, C. Kelly, J. P. Kerry, and D. B. Papkovsky, "High throughput non-destructive assessment of quality and safety of packaged food products using phosphorescent oxygen sensors," *Trends in Food Science and Technology*, 2016, 50: 85–102.

[11] N. Borchert, A. Hempel, H. Walsh, J. P. Kerry, and D. B. Papkovsky, "High throughput quality and safety assessment of packaged green produce using two optical oxygen sensor based systems," *Food Control*, 2012, 28(1): 87–93.

[12] R. I. Dmitriev and D. B. Papkovsky, "*Quenched-phosphorescence Detection of Molecular Oxygen: Applications in Life Sciences*," Cambridge: Royal Society of Chemistry, 2018, 11.

[13] D. Badocco, A. Mondin, and P. Pastore, "Determination of thermodynamic parameters from light intensity signals obtained from oxygen optical sensors," *Sensors and Actuators B: Chemical*, 2012, 163(1): 165–170.

[14] C. S. Chu and C. Y. Chuang, "Highly sensitive fiber-optic oxygen sensor based on palladium tetrakis (4-carboxyphenyl)porphyrin doped in ormosil," *Journal of Luminescence*, 2014, 154: 475–478.

[15] N. Fallahi, P. Ijadi Maghsoodi, M. Habibi, H. Zare-Behtash, M. H. Majlesara, and E. Heydari, "Hybrid dissolved-oxygen and temperature sensing: a nanophotonic probe for real-time monitoring of chlorella algae," *Sensors*, 2021, 21(19): 6553.

[16] C. S. Chu, Y. L. Lo, and T. W. Sung, "Review on recent developments of fluorescent oxygen and carbon dioxide optical fiber sensors," *Photonic Sensors*, 2011, 1: 234–250.

[17] A. Singh, P. Mahajan, A. Sharma, A. Ahmed, S. Verma, B. Padha, *et al.*, "A paper-based colorimetric sensor for highly sensitive and selective detection of multi-metal ions in water," *Brazilian Journal of Physics*, 2022, 52(4): 120.

[18] J. Gupta, S. Arya, S. Verma, A. Singh, A. Sharma, B. Singh, *et al.*, "Performance of template-assisted electrodeposited copper/cobalt bilayered nanowires as an efficient glucose and uric acid senor," *Materials Chemistry and Physics*, 2019, 238: 121969.

[19] C. Kelly, D. Yusufu, I. Okkelman, S. Banerjee, J. P. Kerry, A. Mills, *et al.*, "Extruded phosphorescence based oxygen sensors for large-scale packaging applications," *Sensors and Actuators B: Chemical*, 2020, 304: 127357.

[20] E. Cirulnick, H. Zhang, and D. Klotzkin, "Optical oxygen sensors with improved lifetime incorporating Titania beads and polydimethylsiloxane coatings," *Photonic Sensors*, 2022, 12: 68–73.

[21] T. Okada and M. Kaneko, "*Molecular Catalysts for Energy Conversion*," Heidelberg: Springer, 2008: 185.

[22] D. B. Papkovsky, A. V. Zhdanov, A. Fercher, R. I. Dmitriev, and J. Hynes, *Phosphorescent Oxygen-Sensitive Probes*, Ireland: Springer, 2012: 1–21.

[23] N. Bhalla, P. Jolly, N. Formisano, and P. Estrela, "Introduction to biosensors," *Essays in Biochemistry*, 2016, 60(1): 1–8.

[24] L. C. Chen, E. Wang, C. S. Tai, Y. C. Chiu, C. W. Li, Y. R. Lin, *et al.*, "Improving the reproducibility, accuracy, and stability of an electrochemical biosensor platform for point-of-care use," *Biosensors and Bioelectronics*, 2020, 155: 112111.

[25] C. S. Chu, K. Z. Lin, and Y. H. Tang, "A new optical sensor for sensing oxygen based on phase shift detection," *Sensors and Actuators B: Chemical*, 2016, 223: 606–612.

[26] J. P. Sullivan and T. Liu, *Pressure and Temperature Sensitive Paints*, Berlin: Springer, 2005: 129–153.

[27] E. Heydari, J. AmirAhmadi, N. Ghazyani, G. Bai, H. Zare-Behtash, and M. MajlesAra, "Dual-mode nanophotonic upconversion oxygen sensors," *Nanoscale*, 2022, 14(36): 13362–13372.

[28] F. C. O'Mahony, T. C. O'Riordan, N. Papkovskaia, J. P. Kerry, and D. B. Papkovsky, "Non-destructive assessment of oxygen levels in industrial modified atmosphere packaged cheddar cheese," *Food Control*, 2006, 17(4): 286–292.

[29] A. W. Hempel, M. G. O'Sullivan, D. B. Papkovsky, and J. P. Kerry, "Use of smart packaging technologies for monitoring and extending the shelf-life quality of modified atmosphere packaged (MAP) bread: application of intelligent oxygen sensors and active ethanol emitters," *European Food Research and Technology*, 2013, 237: 117–124.

[30] D. B. Papkovsky, N. Papkovskaia, A. Smyth, J. Kerry, and V. I. Ogurtsov, "Phosphorescent sensor approach for non-destructive measurement of oxygen in packaged foods: optimisation of disposable oxygen sensors and their characterization over a wide temperature range," *Analytical Letters*, 2000, 1755–1777.

[31] A. W. Hempel, M. G. O'sullivan, D. B. Papkovsky, and J. P. Kerry, "Assessment and use of optical oxygen sensors as tools to assist in optimal product component selection for the development of packs of ready-to-eat mixed salads and for the non-destructive monitoring of in-pack oxygen levels using chilled storage," *Foods*, 2013, 2(2): 213–224.

[32] C. A. Kelly, M. Cruz-Romero, J. P. Kerry, and D. P. Papkovsky, "Assessment of performance of the industrial process of bulk vacuum packaging of raw meat with nondestructive optical oxygen sensing systems," *Sensors*, 2018, 18(5): 1395.

[33] D. Airado-Rodríguez, J. Skaret, and J. P. Wold, "Assessment of the quality attributes of cod caviar paste by means of front-face fluorescence spectroscopy," *Journal of Agricultural and Food Chemistry*, 2010, 58(9): 5276–5285.

[34] H. Mohamadi Monavar, N. K. Afseth, J. Lozano, R. Alimardani, M. Omid, and J. P. Wold, "Determining quality of caviar from Caspian Sea based on Raman spectroscopy and using artificial neural networks," *Talanta*, 2013, 111: 98–104.

[35] P. Bronzi, M. Chebanov, J. T. Michaels, Q. Wei, H. Rosenthal, and J. Gessner, "Sturgeon meat and caviar production: Global update 2017," *Journal of Applied Ichthyology*, 2019, 35(1): 257–266.

[36] S. Czesny, K. Dabrowski, J. E. Christensen, J. Van Eenennaam, and S. Doroshov, "Discrimination of wild and domestic origin of sturgeon ova based on lipids and fatty acid analysis," *Aquaculture*, 2000, 189(1–2): 145–153.

[37] M. Al-Holy, Y. Wang, J. Tang, and B. Rasco, "Dielectric properties of salmon (Oncorhynchus keta) and sturgeon (Acipenser transmontanus) caviar at radio frequency (RF) and microwave (MW) pasteurization frequencies," *Journal of Food Engineering*, 2005, 70(4): 564–570.

[38] G. Altug and Y. Bayrak, "Microbiological analysis of caviar from Russia and Iran," *Food Microbiology*, 2003, 20(1): 83–86.

[39] N. M. Asl, H. Ahari, A. A. M. Moghanjoghi, and S. Paidari, "Assessment of nanochitosan packaging containing silver NPs on improving the shelf life of caviar (Acipenser persicus) and evaluation of nanoparticles migration," *Journal of Food Measurement and Characterization*, 2021, 15: 5078–5086.

[40] A. Hempel, D. Papkovsky, and J. Kerry, "Use of optical oxygen sensors in non-destructively determining the levels of oxygen present in combined vacuum and modified atmosphere packaged pre-cooked convenience-style foods and the use of ethanol emitters to extend product shelf-life," *Foods*, 2013, 2(4): 507–520.

[41] A. Mills, "Oxygen indicators and intelligent inks for packaging food," *Chemical Society Reviews*, 2005, 34(12): 1003–1011.

[42] A. Mills, K. Lawrie, J. Bardin, A. Apedaile, G. A. Skinner, and C. O'Rourke, "An O_2 smart plastic film for packaging," *Analyst*, 2012, 137(1): 106–112.

[43] E. Marasca, D. Greetham, S. D. Herring, and I. D. Fisk, "Impact of nitrogen flushing and oil choice on the progression of lipid oxidation in unwashed fried sliced potato crisps," *Food Chemistry*, 2016, 199: 81–86.

[44] C. A. Kelly, E. Santovito, M. Cruz-Romero, J. P. Kerry, and D. P. Papkovsky, "Application of O_2

sensor technology to monitor performance of industrial beef samples packaged on three different vacuum packaging machines," *Sensors and Actuators B: Chemical*, 2020, 304: 127338.

[45] C. Toncelli, O. V. Arzhakova, A. Dolgova, A. L. Volynskii, N. F. Bakeev, J. P. Kerry, *et al.*, "Oxygen-sensitive phosphorescent nanomaterials produced from high-density polyethylene films by local solvent-crazing," *Analytical Chemistry*, 2014, 2(38): 8035–8041.

[46] K. Lee, S. Baek, D. Kim, and J. Seo, "A freshness indicator for monitoring chicken-breast spoilage using a Tyvek® sheet and RGB color analysis," *Food Packaging and Shelf Life*, 2019, 19: 40–46.

[47] W. Cai, J. Wei, Y. Chen, X. Dong, J. Zhang, F. Bai, *et al.*, "Effect of low-temperature vacuum heating on physicochemical properties of sturgeon (Acipenser gueldenstaedti) fillets," *Journal of the Science of Food and Agriculture*, 2020, 100(12): 4583–4591.

[48] A. Lopez, F. Bellagamba, E. Tirloni, M. Vasconi, S. Stella, C. Bernardi, *et al.*, "Evolution of food safety features and volatile profile in white sturgeon caviar treated with different formulations of salt and preservatives during a long-term storage time," *Foods*, 2021, 10(4): 850.

[49] Q. B. Lin, B. Li, H. Song, and H. J. Wu, "Determination of silver in nano-plastic food packaging by microwave digestion coupled with inductively coupled plasma atomic emission spectrometry or inductively coupled plasma mass spectrometry," *Food Additives, and Contaminants: Part A*, 2011, 28(8): 1123–1128.

[50] L. Perring and M. Basic-Dvorzak, "Determination of total tin in canned food using inductively coupled plasma atomic emission spectroscopy," *Analytical and Bioanalytical Chemistry*, 2002, 374: 235–243.